Comparative analysis of Parkinson's disease–associated genes in mice reveals altered survival and bioenergetics of Parkin-deficient dopamine neurons

Received for publication, October 17, 2017, and in revised form, April 23, 2018 Published, Papers in Press, April 26, 2018, DOI 10.1074/jbc.RA117.000499

Nicolas Giguère[‡§1,2,3], **Consiglia Pacelli**[¶1,3], **Caroline Saumure**[‡§], **Marie-Josée Bourque**[‡§], **Diana Matheoud**[§‖], **Daniel Levesque**[**‡‡], **Ruth S. Slack**[§§], **David S. Park**[§§], and **Louis-Éric Trudeau**[‡§‡‡¶¶4]

*From the Departments of [‡]Pharmacology and Physiology and [§]Neurosciences, [¶¶]Central Nervous System Research Group (GRSNC), Faculty of Medicine, Université de Montréal, Québec, Montreal H4T 1J4, Canada, the [¶]Department of Clinical and Experimental Medicine, University of Foggia, Foggia 71122, Italy, the [‖]Centre de Recherche du Centre Hospitalier de l'Université de Montréal (CRCHUM), Québec, Montreal H2X 0A9, Canada, the **Faculty of Pharmacy, Université de Montréal, Québec, Montreal H4T 1J4, Canada, the [‡‡]Groupe de Recherche Universitaire sur le Médicament (GRUM), Montréal, Québec H3C 3J7, Canada, and the [§§]Department of Cellular and Molecular Medicine, University of Ottawa, Ottawa, Ontario K1M 8M5, Canada*

Edited by Paul E. Fraser

Many mutations in genes encoding proteins such as Parkin, PTEN-induced putative kinase 1 (PINK1), protein deglycase DJ-1 (DJ-1 or PARK7), leucine-rich repeat kinase 2 (LRRK2), and α-synuclein have been linked to familial forms of Parkinson's disease (PD). The consequences of these mutations, such as altered mitochondrial function and pathological protein aggregation, are starting to be better understood. However, little is known about the mechanisms explaining why alterations in such diverse cellular processes lead to the selective loss of dopamine (DA) neurons in the substantia nigra (SNc) in the brain of individuals with PD. Recent work has shown that one of the reasons for the high vulnerability of SNc DA neurons is their high basal rate of mitochondrial oxidative phosphorylation (OXPHOS), resulting from their highly complex axonal arborization. Here, we examined whether axonal growth and basal mitochondrial function are altered in SNc DA neurons from Parkin-, Pink1-, or DJ-1–KO mice. We provide evidence for increased basal OXPHOS in Parkin-KO DA neurons and for reduced survival of DA neurons that have a complex axonal arbor. The surviving smaller neurons exhibited reduced vulnerability to the DA neurotoxin and mitochondrial complex I inhibitor MPP+, and this reduction was associated with reduced expression of the DA transporter. Finally, we found that glial cells play a role in the reduced resilience of DA neurons in these mice and that WT Parkin overexpression rescues this phenotype. Our results provide critical insights into the complex relationship between mitochondrial function, axonal growth, and genetic risk factors for PD.

This work was supported in part by a grant from the Krembil Foundation and the Brain Canada Foundation (to R. S., D. P., and L.-E. T.), the Canadian Institutes of Health Research, and by a pilot project grant from Parkinson Society Canada. The authors declare that they have no conflicts of interest with the contents of this article.

This article contains Figs. S1–S5.

[1] Both authors contributed equally to this work.

[2] Recipient of salary support from Fonds du Québec en Recherche, Santé (FRQS).

[3] Recipients of salary support from Parkinson Society Canada.

[4] To whom correspondence should be addressed: Dept. of Pharmacology and Physiology, Faculty of Medicine, Université de Montréal, C.P. 6128, Succursalle Centre-Ville, Montréal, Québec H3T 3J7, Canada. Tel.: 514-343-5692; E-mail: louis-eric.trudeau@umontreal.ca.

In PD,[5] chronic progressive loss of SNc DA neurons leads to some of the characteristic motor symptoms of the disease. Over the past years, many mutations in genes coding for proteins such as the E3 ubiquitin ligase Parkin, PTEN-induced putative kinase 1 (Pink1), protein deglycase DJ-1, leucine-rich repeat kinase 2 (LRRK2), and α-synuclein have been linked to familial forms of the disease.

Although the mechanisms underlying the effects of these mutations, such as alteration in mitochondrial function, mitophagy, lysosomal and proteasome function, and protein aggregation, are slowly starting to be better understood (1), little is known about the reason why alterations in such ubiquitous cellular mechanisms lead to selective loss of sub-populations of neurons, including SNc DA neurons. An emerging hypothesis suggests that the selective vulnerability of DA neurons and other cell groups in PD can be explained in large part by the fact that they establish an unusually complex axonal arborization (2–4). This characteristic has been associated with particularly high demands in ATP needed to sustain neurotransmission along profuse axons (5–8).

Arguing in favor of this hypothesis, recent work showed that SNc DA neurons have a higher basal rate of mitochondrial OXPHOS and ATP production and a smaller reserve capacity compared with less vulnerable DA neurons of the ventral tegmental area (VTA) (9), characteristics that appear to be the result of the highly complex axonal arborization of these neurons and that are also associated with a high level of oxidative stress. Based on these results, a question that arises is whether bioenergetic parameters or axon growth are perturbed in genetic mouse models of PD. Here, we examined primary SNc and VTA DA neurons obtained from Parkin-, Pink1-, or DJ-1–KO mice. We found *in vitro* that basal survival, axonal

[5] The abbreviations used are: PD, Parkinson's disease; DA, dopamine; DAT, dopamine transporter; DIV, days *in vitro*; ECAR, extracellular acidification rate; OCR, oxygen consumption rate; OXPHOS, oxidative phosphorylation; SNc, substantia nigra par compacta; VTA, ventral tegmental area; RCR, respiratory control ratio; MPP+, 1-methyl-4-phenylpyridinium ion; MPTP, 1-methyl-4-phenyl-1,2,3,6-tetrahydropyrindine; mito, mitochondria; DAPI, 4′,6-diamidino-2-phenylindole; AAV, adeno-associated virus; TH, tyrosine hydroxylase; RFP, red fluorescent protein; FUDR, 5-fluoro-2′-deoxyuridine.

growth, and mitochondrial function are altered in SNc DA neurons from Parkin-KO mice but not from Pink1- or DJ-1–KO mice, resulting in an increased oxygen consumption rate (OCR) but lower ATP content. We also found that astrocytes from Parkin-KO mice had a slower growth rate and lower OCR and that their replacement with WT astrocytes abolished the reduction in basal survival observed in Parkin-KO mouse SNc DA neurons. Finally, we show that overexpression of WT Parkin rescues the survival, axonal morphology, and bioenergetics of SNc Parkin-KO mouse cultures. Our data provide new insights in the complex relationship between cellular bioenergetics, axonal development, and survival of DA neurons in Parkin-, Pink1-, and DJ-1–KO mouse models of PD, highlighting a critical role for Parkin.

Results

SNc DA neurons in Parkin- but not PINK1- or DJ-1–KO PD mouse models show altered basal survival and growth

Experiments were performed using a mouse primary culture system, including DA neurons microdissected from the SNc and VTA of newborn Parkin-, Pink1-, or DJ-1–KO mice. The neurons were grown on a supporting monolayer of astrocytes of the corresponding genotype. As reported previously (9), in such cultures, WT SNc DA neurons show increased basal respiration, increased ATP production, and a larger axonal arborization compared with WT VTA DA neurons (Fig. S1).

We first evaluated the rate of spontaneous loss of DA neurons *in vitro* over a period of 11 days as an index of the neurons' basal resilience. At 11 DIV, a time point at which DA neurons are mature at the morphological and metabolic levels, we found that Parkin-KO SNc DA neurons showed a pronounced rate of spontaneous degeneration, with 56% more cell loss compared with WT SNc DA neurons (Fig. 1*A*). We did not observe any similar enhancement of SNc DA neuron loss in Pink1-KO or DJ-1–KO neurons (Fig. 1, *B* and *C*) or in VTA cultures from any of the three genotypes (Fig. 1, *D–F*). Interestingly, there was also no change in survival at an earlier time point in SNc Parkin-KO culture (5DIV, Fig. S2*A*), arguing for the need of sustained stress for this increased vulnerability to be revealed. We next examined axonal arborization size in the remaining Parkin-KO mouse SNc DA neurons at 11 DIV and found that it was 40% smaller compared with WT (Fig. 1, *G* and *H*), with no change in Parkin-KO mouse VTA neurons. Again, we did not observe any differences between Pink1-WT and -KO mouse DA neurons, between DJ-1–WT and –KO DA neurons (Fig. 1, *I* and *J*), or at an earlier time point in Parkin-WT mouse neurons *versus* KO mouse DA neurons (Fig. S2*B*). These results suggest that Parkin-KO mouse SNc DA neurons have a higher intrinsic vulnerability and that the most arborized DA neurons are degenerating preferentially or, alternatively, that axonal development is slowed in these neurons after prolonged development *in vitro*.

Parkin but not PINK1- or DJ-1–KO DA neurons show altered mitochondrial function

Because recent work has provided evidence for a close relationship between survival, axonal arborization size, and mitochondrial bioenergetics in DA neurons (9), we next evaluated mitochondrial OXPHOS by measuring cellular respiration. At 10 DIV, basal and maximal (uncoupled with CCCP) oxygen consumption rates (OCR) were measured in living neurons. The respiratory control ratio (RCR), corresponding to the ratio between basal and maximal OCR, was also determined to estimate the respiratory reserve capacity. We found that basal OCR was significantly increased by 50% in Parkin-KO mouse SNc DA neurons compared with WT (Fig. 2*A*). However, maximal OCR or the RCR were unchanged in these neurons (Fig. 2*A*). OCR was unchanged in SNc DA neurons from Pink1-KO mice or DJ-1–KO mice (Fig. 2, *B* and *C*) or at 5 DIV in SNc Parkin-KO mouse culture (Fig. S2*C*). Interestingly, basal OCR was significantly increased by 181% in Parkin-KO mouse VTA DA neurons, accompanied by an increase of maximal OCR of 120%, with no changes in RCR (Fig. 2*D*). OCR was unchanged in VTA DA neurons form Pink1 or DJ-1–KO mice.

Considering previous work suggesting a critical role for Parkin in the turnover of mitochondria (10–12), a possible interpretation of the increase in basal OCR in Parkin-KO mouse DA neurons is that loss of Parkin leads to the presence of dysfunctional mitochondria that are partially uncoupled. If this were the case, a prediction is that the increase in OCR should not be accompanied by an increase in ATP production and could even be accompanied by a decrease in ATP. To test this hypothesis, we measured ATP content in each culture and discovered a significant reduction of 44% in ATP levels in Parkin-KO mouse SNc cultures, with no change in Pink1-KO or DJ-1–KO mouse cultures (Fig. 2, *G–I*). Such a possible uncoupling between OCR and ATP production appears to be particularly exacerbated in Parkin-KO mouse VTA DA neuron cultures, perhaps because more of these neurons survived to this impairment, compatible with their higher resilience in response to oxidative stress (9). Interestingly, contrary to SNc DA neurons (Fig. 3*A*), VTA DA neurons from Parkin-KO mice showed an increase in basal glycolysis (Fig. 3*B*), perhaps representing a compensatory mechanism for impaired mitochondrial function. This was not observed in SNc or VTA neurons from either PINK1- or DJ-1–KO mice (Fig. 3, *C–F*).

Considering our data arguing for defective mitochondrial function in SNc DA neurons from Parkin-KO mice, the distribution and density of mitochondria in DA neurons from this genetic background were also directly examined by infecting cells with a mitochondrially-tagged DsRed protein (DsRed2-mito-lentivirus) (Fig. 4*A*). No significant difference was detected in the density of mitochondria in the soma, axon, or dendrites of SNc DA neurons from Parkin-KO mice compared with WT (Fig. 4*B*).

Parkin-KO mice glia show altered growth, extracellular acidification rate (ECAR), and OCR and influence basal survival of SNc DA neurons

The reduced resilience of SNc DA neurons cultured from Parkin-KO mice could be due to a cell-intrinsic perturbation, to perturbation of non-neuronal cells such as astrocytes or microglia, or a combination of the two. Previous work has indeed demonstrated reduced proliferation of astrocytes, increased density of microglia, and reduced neuroprotective effects of glial-conditioned medium from Parkin-KO mice (13). We therefore evaluated the implication of glial cells in the altered

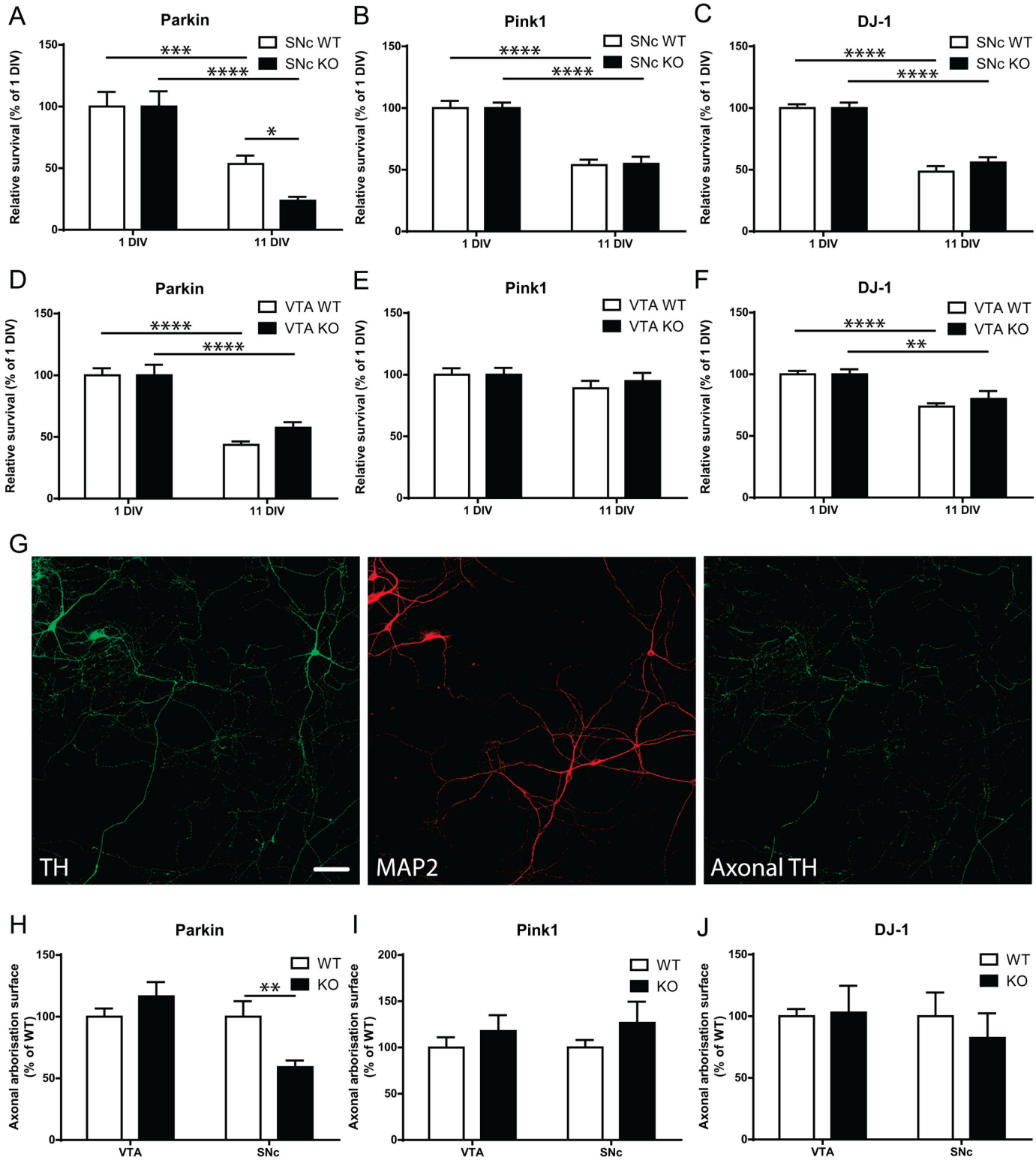

Figure 1. Altered basal survival and axonal arbor size of Parkin but not PINK1 or DJ-1–KO mouse SNc DA neurons. *A–F*, basal survival rate was measured by counting the proportion of DA neurons with a clear round nucleus at 1 DIV that survived until 11 DIV in Parkin-KO mice (*A* and *D*), Pink1-KO mice (*B* and *E*), or DJ-1-KO mice (*C* and *F*) SNc or VTA cultures. The values represent the mean ± S.E., $n = 8–24$ coverslips from at least three different cultures. *, $p < 0.05$; **, $p < 0.01$; ***, $p < 0.001$; ****, $p < 0.0001$. *G–J*, axonal arborization size was measured by removing somatodendritic (MAP2 signal) surface from TH surface in random fields (*G*); *scale bar*, 100 μm. The values obtained were normalized to the number of TH-positive SNc or VTA DA neurons in Parkin (*H*), Pink1 (*I*), and DJ-1 (*J*) cultures. The values represent the mean ± S.E., $n = 13–17$ coverslips from at least three different cultures. **, $p < 0.01$.

survival of the Parkin-KO mouse SNc DA neurons by growing Parkin-KO mouse DA neurons with WT glia. We found that this completely reverted this reduced survival phenotype (Fig. 5*A*). Compatible with previous results (13), there were 33% fewer cells in Parkin-KO mouse cortical glial cultures after 7 DIV, 36% less at 10 DIV, and 39% fewer cells at 10 DIV when a

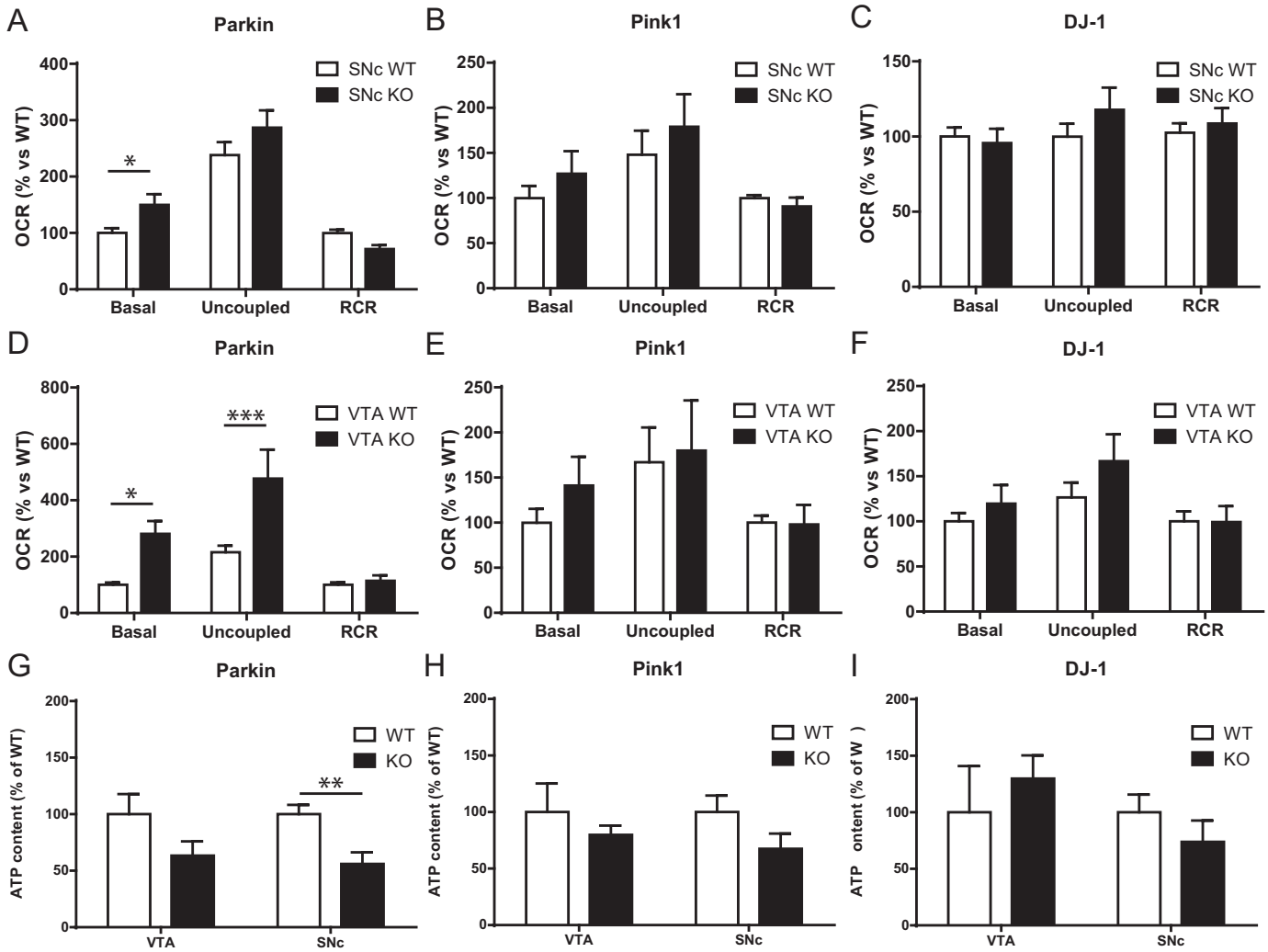

Figure 2. Altered mitochondrial function in Parkin but not PINK1 or DJ-1–KO mouse DA neurons. *A–F*, OCR was measured using an XF24 analyzer from Parkin (*A*), Pink1 (*B*), and DJ-1 (*C*) SNc cultures and from Parkin (*D*), Pink1 (*E*), and DJ-1 (*F*) VTA cultures. Basal OCR, uncoupled OCR in the presence of 0.5 mM CCCP, and the RCR, calculated by dividing uncoupled by basal OCR, were measured. The values represent the mean ± S.E., $n = 7–27$ wells from at least three different cultures. *, $p < 0.05$; ***, $p < 0.001$. *G–I*, ATP content under basal conditions was quantified in SNc and VTA DA neurons from Parkin (*G*), Pink1 (*H*), and DJ-1 (*I*) cultures. Values represent the mean ± S.E., $n = 5–7$ coverslips from at least three different cultures. **, $p < 0.005$.

mitotic inhibitor was added after glial cells reached confluence, conditions that mimicked those used to prepare neuronal cultures (Fig. 5, *B* and *C*). The proliferation of mesencephalic glial cells was similarly reduced (Fig. S3). Glial cells in Parkin-KO mouse cultures were also perturbed at the metabolic level, as revealed by the fact that basal OCR was reduced by 24% and maximal OCR by 25%, with no change in RCR (Fig. 5*D*). In addition, basal glycolysis was increased by 52% (Fig. 5*E*), and no change was observed in ATP levels (Fig. 5*F*), suggesting the possibility of a compensation by glycolysis of the reduced OXPHOS. Similar measurements performed in Pink1-KO mice and DJ-1–KO cultures revealed a decreased basal and maximal OCR in glial cells from Pink1-KO mice but not DJ-1–KO mice, with no changes in any other measurements (Fig. S4).

Vulnerability to the neurotoxin MPP+ is altered in Parkin, DJ-1, but not PINK1-KO mouse SNc DA neurons

The reduced basal survival of SNc DA neurons from Parkin-KO mice (Fig. 1*A*) together with the observation of reduced axonal arborization size (Fig. 1*H*) in these surviving neurons suggest the possibility that the surviving smaller neurons might be more resilient, as in a recent model (4, 9). To test this possibility, we next examined the vulnerability of DA neurons at 10 DIV to cellular stress induced by the DA neuron-specific neurotoxin and mitochondrial complex I inhibitor MPP+. Interestingly, the surviving SNc DA neurons from the Parkin-KO mouse cultures were significantly less vulnerable to MPP+ (Fig. 6*A*). No change in vulnerability was observed in SNc DA neurons from Pink1-KO mice (Fig. 6*B*). Finally, SNc DA neurons from DJ-1–KO mice were to the contrary more vulnerable to MPP+ (Fig. 6*C*). Compatible with previous work showing a higher resilience of VTA DA neurons, MPP+ caused much smaller cell loss in VTA DA neurons, and no difference was found between genotypes (Fig. 6, *D–F*).

Reduced DA transporter expression in surviving SNc DA neurons in Parkin-KO mice

Although reduced vulnerability of surviving SNc DA neurons from Parkin-KO mice could be due to a number of factors, an obvious possibility is that reduced toxicity could be due to

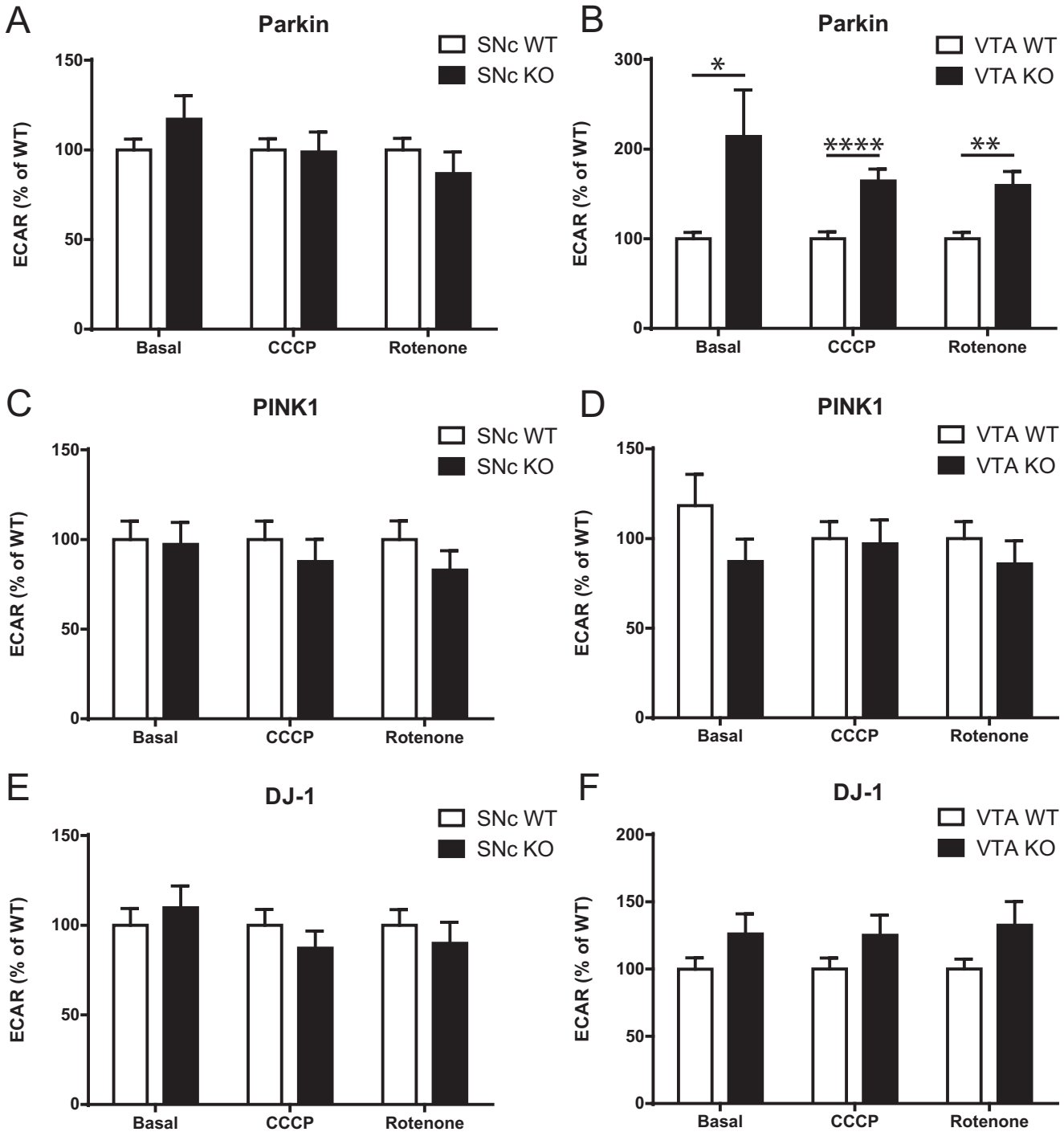

Figure 3. *A–F*, ECAR was measured using an XF24 analyzer from Parkin (*A*), Pink1 (*C*), and DJ-1 (*E*)-KO mouse SNc cultures and from Parkin (*B*), Pink1 (*D*), and DJ-1 (*F*) VTA-KO mouse cultures. ECAR under basal conditions (*Basal*), in the presence of 0.5 mM CCCP (*CCCP*), and in the presence of 1 μM rotenone (*Rotenone*) were measured. The values represent the mean ± S.E., $n = 17–27$ wells from at least three different cultures. *, $p < 0.05$; **, $p < 0.01$; ****, $p < 0.0001$.

lower levels of the DA transporter (DAT), which is the route of entry of MPP+ in DA neurons (14). We measured DAT density using a radio ligand assay and found that the surviving DA neurons indeed showed 60% less DAT compared with WT SNc DA neurons (Fig. 7*A*). Also arguing in favor of this hypothesis, vulnerability to DAT-independent toxic treatments such as hydrogen peroxide (Fig. 7*B*) or the complex I blocker rotenone (Fig. 7*C*) was similar in Parkin-KO mice and WT SNc DA neuron cultures. Finally, vulnerability to MPP+ of Parkin-KO mouse SNc DA neuron growth together with WT glia, conditions that prevent the loss of SNc DA neurons, was similar to that of WT SNc DA neurons (Fig. 7*D*).

Partial rescue of Parkin-KO mouse SNc DA neurons by WT Parkin overexpression

Finally, to further strengthen the idea that the reduced basal survival, axonal length, and increased basal OCR in SNc DA neurons from Parkin-KO mice is a direct consequence of the

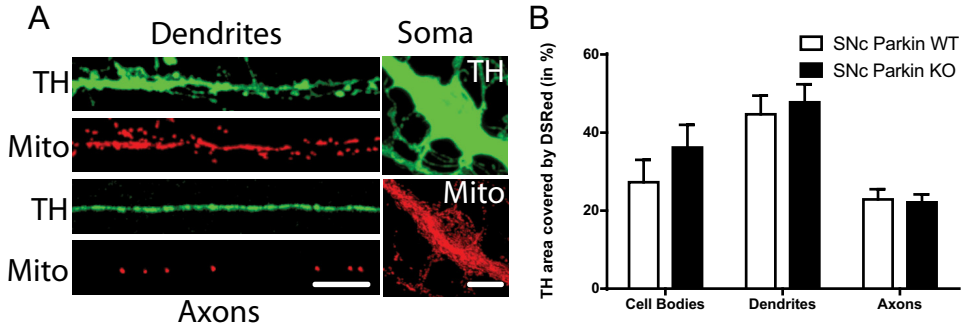

Figure 4. No change in mitochondrial density in Parkin-KO mouse SNc DA neurons. *A* and *B,* SNc DA neurons were infected with DsRed2-mito at the time of plating. The density of mitochondria (*A*) was measured in TH-positive neurons using confocal microscopy. *Scale bar,* 10 μm. *B,* proportion of TH signal covered by DSRed in cell bodies, dendrites, and axons. The values represent the mean ± S.E., $n = 20–26$ neurons from at least three different cultures.

loss of Parkin expression, we overexpressed WT Parkin using an AAV vector (Fig. 8*A*). We found that the basal survival of SNc DA Parkin-KO mouse neurons was partially rescued by Parkin overexpression (Fig. 8*B*) and that their axonal length and basal OCR was also back to WT levels (Fig. 8, *C* and *D*), without changing maximal OCR or RCR (Fig. 8, *E* and *F*).

Discussion

Since the discovery of the first human mutations causing familial forms of Parkinson's disease, extensive work has been performed to identify the mechanisms by which loss- or gain-of-function of gene products, including Parkin, Pink1, DJ-1, LRRK2, and α-synuclein, trigger the disease process. One of the approaches used has been to create knockout animals in species such as flies and mice in the hope of obtaining valid models of the disease. Unfortunately, in mice, constitutive-KO of these genes typically does not lead to age-dependent loss of DA neurons *in vivo* (15–17). A possible explanation could be that it is difficult to model age-dependent neurodegeneration in species with a short life span or that mice need to be exposed to a second hit to trigger the disease. Another possibility is that the cumulative burden of oxidative stress in mouse DA neurons is not sufficiently high to lead to cell loss. Whatever the case may be, using these models is still of interest to examine some of the early stages of the disease, prior to cell loss. Indeed, various cellular and subcellular dysfunctions have been reported in such models during the past decade (18–22). In this work, we aimed to determine whether basal resilience and parameters linked to cellular bioenergetics such as mitochondrial OXPHOS and axonal arborization size are altered in primary cultures prepared from Parkin-, Pink1-, or DJ-1–KO mice.

Morphological and bioenergetic alterations in Parkin-KO mouse SNc cultures

We discovered that basal survival *in vitro*, axonal growth, and mitochondrial functions are altered in SNc DA neurons from Parkin-KO mice, with little if any changes in Pink1-KO mice or DJ-1–KO mice. Our finding of reduced basal survival of SNc DA neurons in Parkin-KO mice argues that SNc DA neurons in these mice have a higher basal vulnerability to cellular stress, a conclusion that is in keeping with previous results (9, 23, 24). Interestingly, we found that the subset of SNc DA neurons that survived up to 11 DIV in Parkin-KO mouse cultures possessed a smaller axonal arborization and produced less ATP, findings that are compatible with previous work proposing that cellular bioenergetics are directly related to axon length and to vulnerability (9). Further experiments directly evaluating the links between ATP levels and axon growth in DA neurons would help establish more direct links between these parameters. Our observation of reduced axonal arborization size is also in line with recent work showing reduced complexity of neuronal processes in induced pluripotent stem cell-derived human neurons carrying Parkin mutations (25). However, somewhat surprisingly, surviving Parkin-KO mouse SNc DA neurons at 10 days *in vitro* showed higher basal OCR, suggesting an uncoupling between oxygen consumption and ATP production. This observation could be the result of the accumulation of damaged mitochondria and as such would be compatible with previous work showing mitochondrial dysfunction in Parkin-KO mouse mutant *Drosophila* (26). However, no increase in OCR was reported in mouse cortical or striatal primary cultures or in mesencephalic post-nuclear supernatants prepared from adult Parkin-KO mice (27). Because such cultures do not contain any DA neurons and because OCR measurements from mesencephalic post-nuclear supernatants are necessarily contaminated by non-DA neurons and other cells, it is possible that a change in OCR occurring principally in DA neurons may have been missed in these previous studies.

Impaired mitochondrial function in SNc Parkin-KO cultures

Considering that Parkin is normally recruited by Pink1 to damaged mitochondria to initiate mitophagy, it is possible that the increase in OCR with a reduction in ATP levels that we observed in residual SNc DA neurons after 10 days *in vitro* is the result of the accumulation of malfunctioning, uncoupled mitochondria. Although we cannot exclude this possibility, our observation of a lack of change in mitochondrial density, evaluated with Mito-DsRed, does not provide support for such an interpretation. One possibility is that other mechanisms compensate for the lack of Parkin-mediated mitophagy. Such mechanisms could either get rid of some of the damaged mitochondria in a Parkin-independent manner and/or slow down the production of new mitochondria, explaining the lack of change of total mitochondrial density. Although recent work suggests that the rate of mitophagy in axons may be very limited (28), additional experiments directly quantifying mitochondrial turnover could help clarify this issue. Nonetheless, the increase

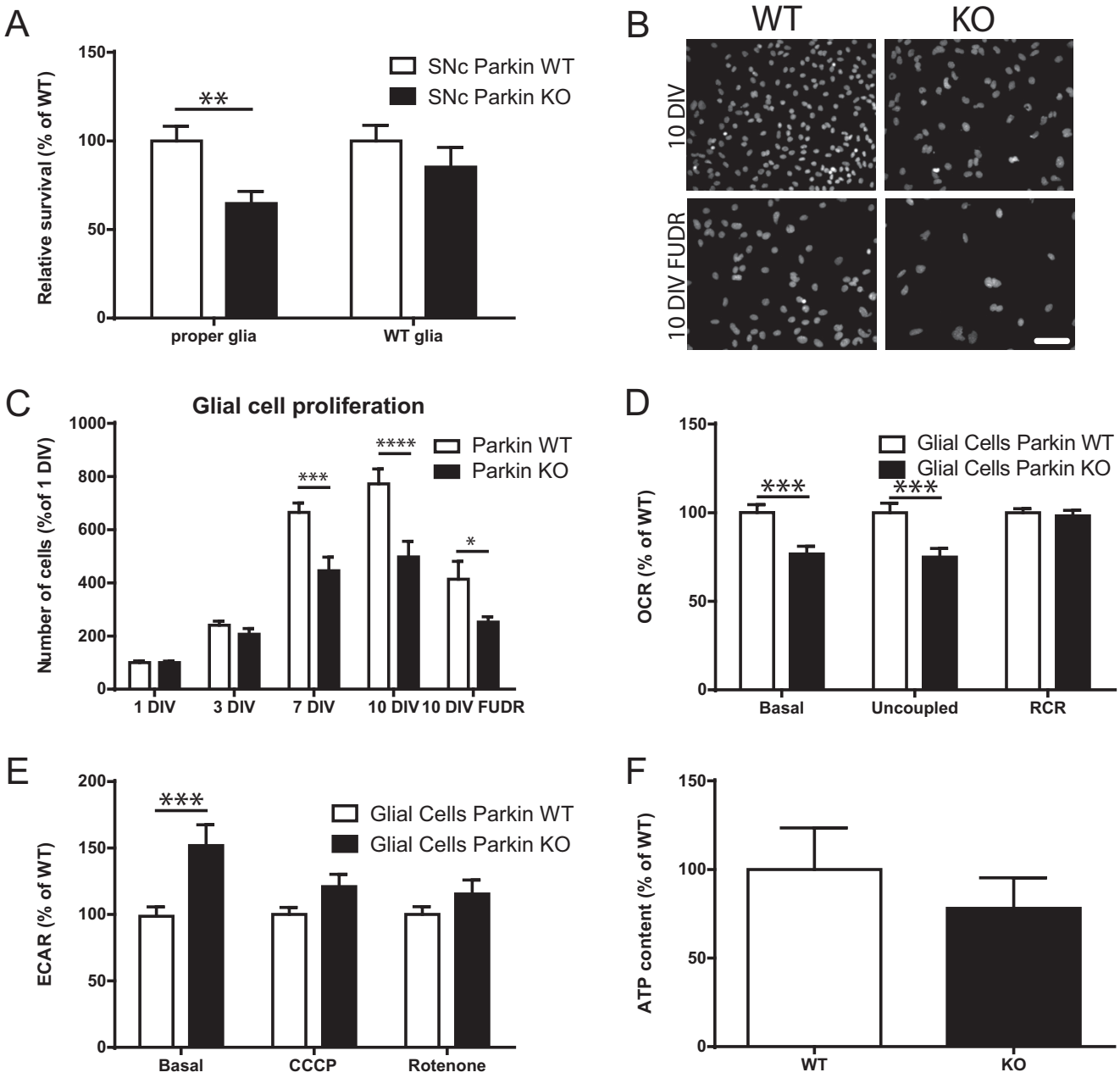

Figure 5. Parkin-KO mice glial cell dysfunction is implicated in basal survival of Parkin-KO mouse SNc DA neurons. *A,* SNc Parkin-KO mice and WT DA neurons were grown on corresponding or WT glial cells, and survival was measured by counting the proportion of DA neurons with a clear round nucleus. The values represent the mean ± S.E., $n = 18–31$ coverslips from at least three different cultures. **, $p < 0.01$. *B* and *C,* Parkin-KO mouse glial cells were grown on coverslips for 1, 3, 7, and 10 DIV. In another group of coverslips, the mitotic inhibitor FUDR was added once glial cells reached confluence as per the procedure typically used to prepare neuronal cultures. The number of glial cells was measured by DAPI staining. *Scale bar,* 100 μm. The values represent the mean ± S.E., $n = 8–12$ coverslips from at least three different cultures. *, $p < 0.05$; ***, $p < 0.001$; ****, $p < 0.0001$. *D* and *E,* OCR (*D*) and ECAR (*E*) were measured using an XF24 analyzer from Parkin glial cell cultures. The values represent the mean ± S.E., $n = 16–36$ wells from at least four different cultures. **, $p < 0.01$; ***, $p < 0.001$. *F,* ATP content under basal conditions was quantified in Parkin-KO mouse glial cell cultures. The values represent the mean ± S.E., $n = 6–7$ coverslips from at least three different cultures.

in OCR combined with decreased ATP production argues for malfunctioning mitochondria (9, 22, 29, 30). In this context, the resulting metabolic stress could favor the survival of neurons with smaller bioenergetic needs such as those that have a smaller axonal arborization. Arguing in favor of this interpretation, VTA DA neurons, which are less vulnerable in PD and normally have a smaller axonal arborization than SNc DA neurons (9), did not show altered survival in the absence of Parkin under our experimental conditions. We found that even if they showed a much higher basal OCR, their ATP production and axonal arborization were unchanged. This highlights the higher basal resilience of these neurons. Further experiments quantifying basal reactive oxygen species production and antioxidant defense mechanisms in VTA DA neurons would be helpful to further characterize and explain such resilience.

Our finding of a lack of change in bioenergetics and axonal growth in DA neurons from Pink1- and DJ-1–KO mice is puzzling, especially concerning the implication of Pink1 in mito-

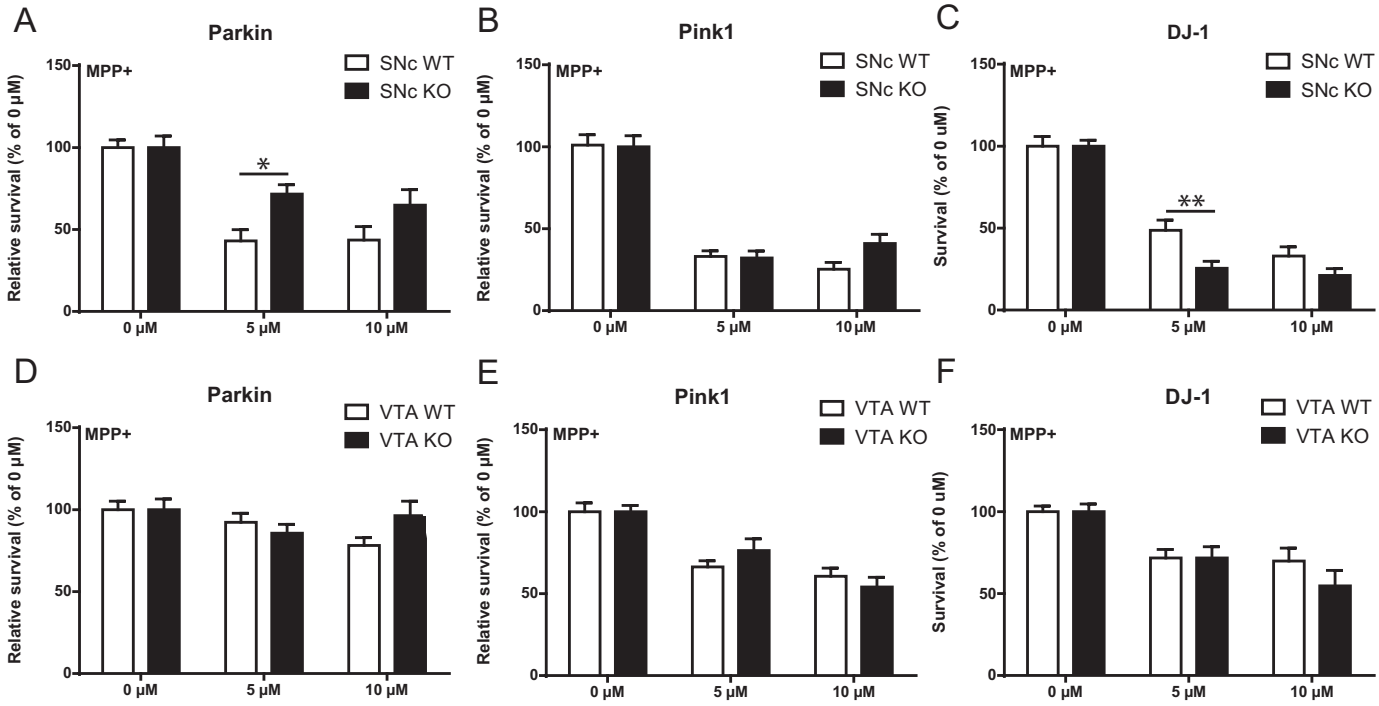

Figure 6. Altered survival to MPP+ of SNc DA neurons in Parkin, DJ-1, but not PINK1-KO cultures. *A–F,* DA neurons were treated with MPP+ (5 and 10 μM, 24 h), and the proportion of surviving neurons was determined by counting the number of TH-positive neurons with a clear round nucleus in SNc cultures prepared from Parkin (*A*), Pink1 (*B*), or DJ-1 (*C*)-KO mice or in VTA cultures (*D–F*). The values represent the mean ± S.E., $n = 12–25$ coverslips from at least three different cultures. *, $p < 0.05$; **, $p < 0.01$.

chondrial quality control, in a common pathway with Parkin. A partial explanation could come from recent work showing that mitochondrial quality control in tissues with elevated metabolic demands such as the brain can be Pink1-independent (31). If this is also the case in our model, this could explain why we only see alterations in Parkin-KO mouse cultures. Except for a recent study reporting age-dependent unilateral loss of SNc DA neurons in a new sub-strain of DJ-1–KO mice (15), there have been no previous reports of altered basal growth and survival of DA neurons in Pink1- or DJ-1–KO mouse lines. However, previous work has reported impaired respiration and increased glycolytic activity in mixed neuronal cultures from the midbrain of Pink1-KO mice (32). The relative abundance of DA neurons in such cultures was not reported, making it unclear whether results reflected the bioenergetic properties of SNc DA neurons. In addition, mitochondrial membrane potential was used to indirectly evaluate OXPHOS, making a comparison with our present results difficult. Concerning DJ-1, previous work using a neuron-like cell line showed reduced OCR and ATP production (33). It is very difficult to compare our findings to such results because of the major morphological and bioenergetic differences between such cell lines and primary DA neurons, in addition to the major difference in cell maturity between the two studies (18 h in the Heo *et al.* study (33) compared with 10 days for the present study). In this study, although increased cell loss was apparent after 11 days in Parkin-KO mouse cultures, we found no change after 5 days. Similarly, loss of Pink1 or DJ-1 might therefore need more time to reveal an increased vulnerability, as suggested by work on aged Pink1-KO mice (34). Further studies evaluating neuronal survival in DA neurons from Pink1- or DJ-1–KO mice after longer time points in culture might thus be useful to determine whether changes in vulnerability do exist but simply need a higher level of cellular stress or time to be revealed.

WT Parkin overexpression rescues morphological and bioenergetic defects in Parkin-KO mouse SNc cultures

Because the KO strain used in this work was constitutive, the increased vulnerability of SNc DA neurons we detected in Parkin-KO mouse cultures could result from changes occurring during embryonic development of the neurons and not be a direct consequence of the lack of Parkin expression in cells. To explore this possibility, we performed a rescue experiment and reintroduced WT Parkin using an AAV vector. We found that such overexpression was sufficient to rescue the changes in basal survival, axonal growth, and mitochondrial OXPHOS in Parkin-KO mouse SNc DA neurons, observations that are compatible with previous work showing that overexpression of WT Parkin is neuroprotective (35, 36). An important limitation of the present rescue experiment is that Parkin expression was driven through a strong CBA promoter, likely leading to expression levels much higher than WT levels (Fig. S5).

Parkin-KO glial cell alterations and implications for neuronal defects

The increased vulnerability of SNc DA neurons we detected in Parkin-KO mouse cultures could result from cell-autonomous alterations, from non-cell–autonomous mechanisms, such as a change in glial cell function, as reported previously (13), or a combination of the two. To explore the implication of astrocytes, cells that play a key role in the trophic support of DA neurons (37, 38), we prepared mixed cultures containing WT

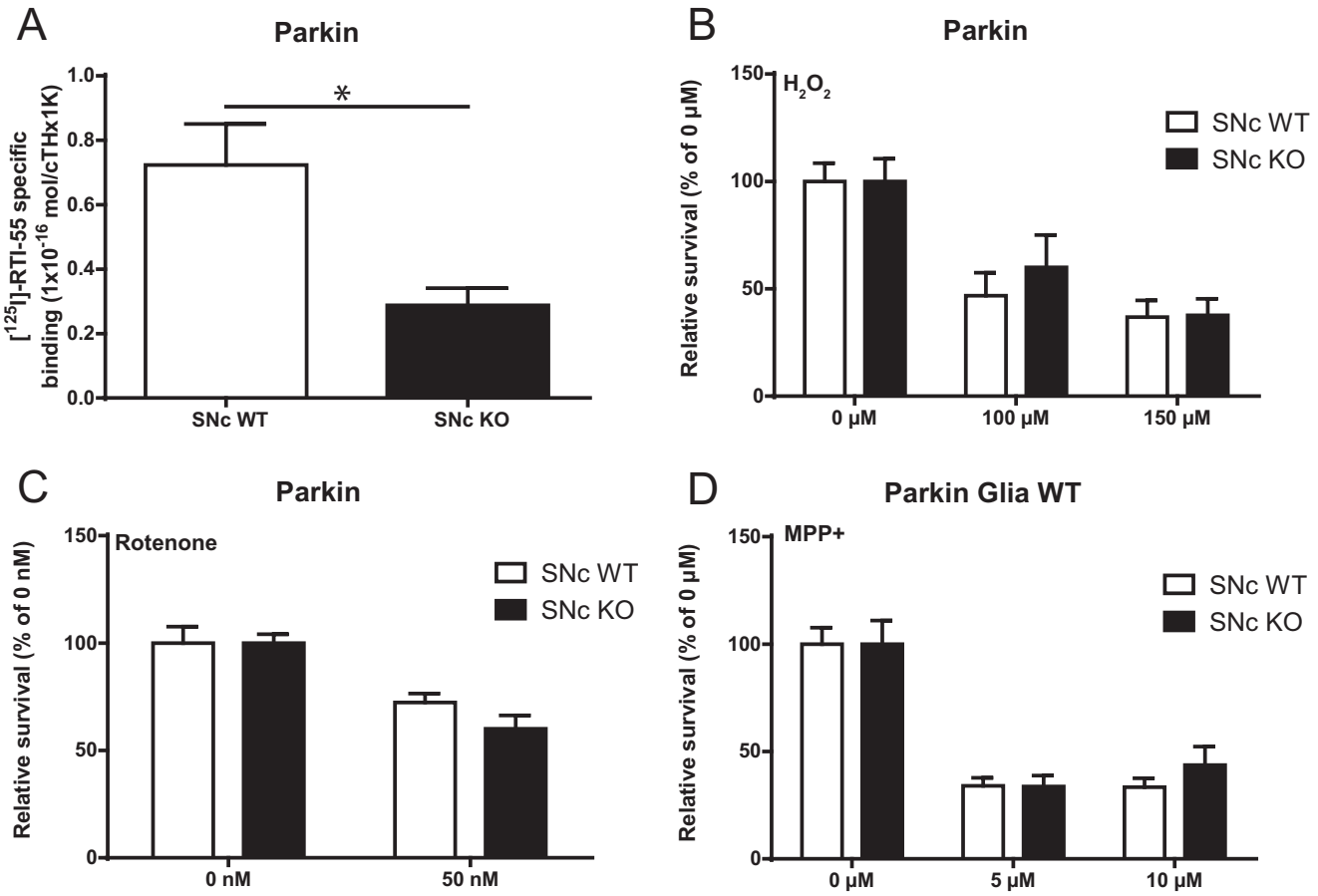

Figure 7. Differential vulnerability to MPP+ of Parkin-KO mouse SNc DA neurons associated with lower DAT expression in surviving neurons. *A,* density of DAT was measured by radioligand assay in Parkin-KO mouse SNc cultures. The values represent the mean ± S.E., $n = 3$ samples from three different cultures. *, $p < 0.05$. *B* and *C,* Parkin-KO mice SNc neurons were treated with H_2O_2 (100 and 150 μM, 24 h) (*B*) or rotenone (50 nM, 72 h) (*C*), and the proportion of surviving neurons was determined by counting the number of TH-positive neurons with a clear round nucleus. The values represent the mean ± S.E., $n = 8–20$ coverslips from at least three different cultures. *D,* Parkin-KO mice SNc cultures under WT glia were treated with MPP+ (5 and 10 μM, 24 h), and the proportion of surviving neurons was determined by counting the number of TH-positive neurons with a clear round nucleus. The values represent the mean ± S.E., $n = 10–20$ coverslips from at least three different cultures.

glia and Parkin-KO mouse DA neurons. In such cultures, we observed no significant differential loss of SNc DA neurons over 10 days *in vitro*, arguing for a major implication of glial cell dysfunction in the reduced survival of SNc DA neurons in cultures prepared from Parkin-KO mice. Compatible with glial cell dysfunction in such mice, we found slower proliferation of Parkin-KO mouse glial cells, an observation that is in line with previous work (13, 39). Such slower proliferation of glial cells (mostly astrocytes) led to a reduced density of such cells at 10 DIV, accompanied by a reduction in OCR, but an increase in glycolysis, with no changes in ATP levels. It is possible that the reduction in glial cell number itself influenced neuronal survival in Parkin-KO mouse cultures. However, we feel that this is unlikely because we found that very large reductions in glial cell density are required to negatively impact DA neuron survival (data not shown). Here, the reduction in glial cell density was modest (~33%) and was not accompanied by a decrease in ATP production. Future work will be required to determine whether the secretion of glial cell-derived neurotrophic factors or the regulation of lactate or pyruvate shuttling is altered in Parkin-KO mouse astrocytes, providing a potential explanation for the reduced survival of SNc DA neurons.

Lower DAT level in surviving Parkin-KO SNc neurons

SNc DA neurons are well-known to be particularly vulnerable to mitochondrial toxins such as MPP+, which enter DA neurons through the DAT (14). DA neurons in Pink1- and DJ-1–KO mice have been reported to be more vulnerable to different toxin models, suggesting increased cell vulnerability (21, 40–45). Surprisingly, this is not the case for Parkin-KO mice (30, 46–49). We therefore also investigated this issue in this study using MPP+, the active metabolite of MPTP. Interestingly, we found increased vulnerability to MPP+ only in SNc DA neurons cultured from DJ-1–KO mice, but not in cultures prepared from Pink1- or Parkin-KO mice, arguing that some of the properties of DJ-1, such as its antioxidant role, is important to prevent toxicity to MPP+, even if it is not necessary for survival up to 11 DIV under our basal culture conditions. Because the MPTP experiments cited previously were performed in adult mice, it is possible that the developing state of our neurons prevented us from seeing such increased vulnerability in Pink1-KO mouse cultures. Surprisingly, in Parkin-KO mouse SNc cultures, the neurons surviving after 10 DIV were actually less vulnerable to MPP+. This could perhaps be due to

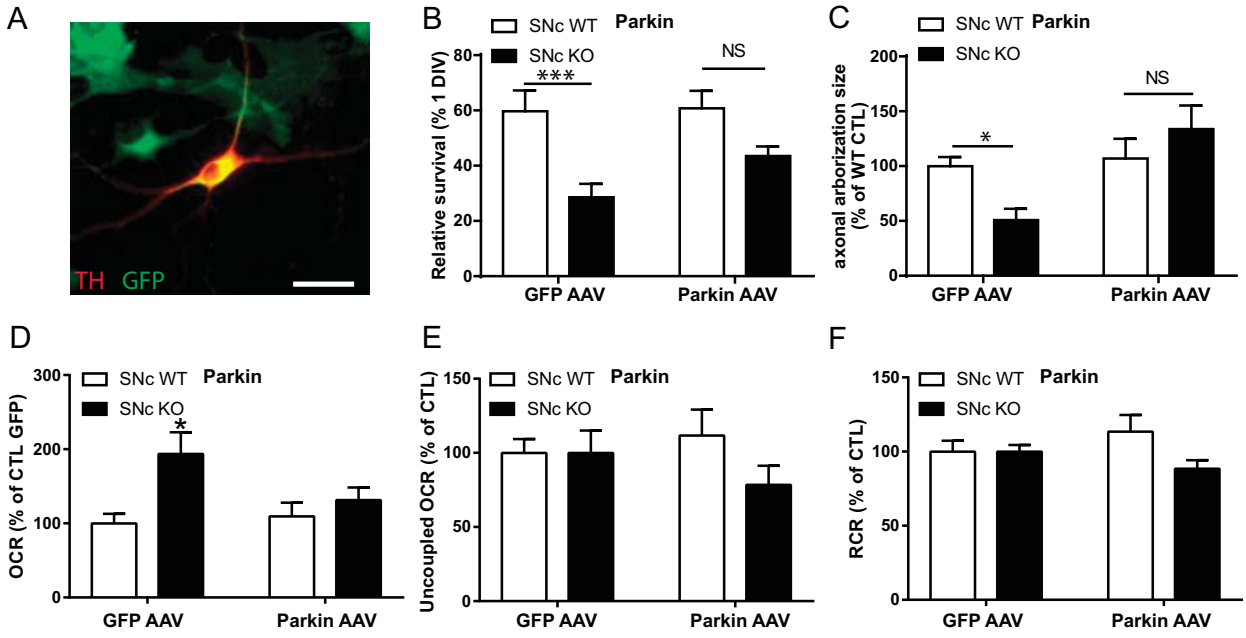

Figure 8. Partial rescue of basal survival, axonal length, and bioenergetics in Parkin-KO mice SNc cultures by AAV overexpression of WT Parkin. *A,* Parkin WT and KO mouse SNc cultures were infected with Parkin WT-GFP AAV or GFP only AAV and cultured for 10 DIV. *Scale bar,* 25 μm. *B,* basal survival rate was measured by counting the proportion of DA neurons with a clear round nucleus at 1 DIV that survived until 10 DIV. *C,* axonal arborization size was measured by removing somatodendritic (MAP2 signal) surface from the TH surface in random fields. Data were normalized to the control condition. The values represent the mean ± S.E., $n = 8–12$ coverslips from at least three different cultures. *, $p < 0.05$; ***, $p < 0.001$. Oxygen consumption rates were measured using an XF24 analyzer. Basal OCR (*D*), uncoupled OCR (*E*) in the presence of 0.5 μM CCCP, and the RCR (*F*), calculated by dividing uncoupled by basal OCR, were measured. Data were normalized to the control condition. The values represent the mean ± S.E., $n = 15–25$ wells from at least six different cultures. *, $p < 0.05$. *NS,* non-significant.

lower expression of DAT in surviving DA neurons, a down-regulation reported previously when this mouse was first characterized (48) and more recently in Parkin mutant human midbrain DA neurons derived from induced pluripotent stem cells (50). Compatible with this, we did observe a lower expression of DAT in Parkin-KO mouse cultures. In addition, we found no change in survival in response to DAT-independent oxidative stress such as that induced by rotenone or H_2O_2. This last finding is in apparent contradiction with previously published data showing that embryonic midbrain DA neurons from Parkin-KO mice show an increased vulnerability to rotenone (51). The different type of cultures used (embryonic *versus* postnatal), density of DA neurons (low *versus* high), age of cultures (7 *versus* 10 DIV), and the different duration of rotenone application are all factors that should be considered to explain such different results. Interestingly, in this study, we found no differential effect of MPP+ on the survival of Parkin-KO mouse DA neurons when Parkin-KO mouse SNc DA neurons were cultured together with WT glia; this finding could be taken to suggest that the differential expression of DAT alone is not sufficient to explain the differential survival of SNc DA neurons to MPP+ in Parkin-KO mouse cultures. However, a more comprehensive explanation is that in Parkin-KO mouse SNc cultures, the impaired functioning of astrocytes leads to the preferential death of highly arborized DA neurons, a population of neurons that are otherwise more vulnerable to cellular stressors in general (9). Because of this differential survival, the remaining SNc DA neurons in Parkin-KO mouse cultures would have lower axonal arborization and reduced DAT expression with consequent reduced vulnerability to MPP+. DAT levels were not quantified in cultures prepared from Pink1-KO or DJ-1–KO mice.

Our data provide new insights into the complex relationship between mitochondrial function, axonal growth, and genetic risk factors linked to PD. Previous work has shown that overexpression of Parkin, Pink1, or DJ-1 in DA neurons is neuroprotective against mitochondrial toxins (35, 36, 52). Such results argue for a direct role of these gene products in regulating the vulnerability of DA neurons. The present results also uncover a role of Parkin in regulating mitochondrial function and OXPHOS in DA neurons. However, our findings also argue for the existence of more indirect roles through an impact on glial cells. Further work will be required to examine whether such changes might be key to explain the heightened vulnerability of SNc DA neurons over multiple decades, as occurs in PD.

Experimental procedures

Animals

All procedures involving animals were conducted in strict accordance with the Guide to Care and Use of Experimental Animals (2nd Ed.) of the Canadian Council on Animal Care. The experimental protocols were approved by the animal ethics committee (CDEA) of the Université de Montréal. Housing was at a constant temperature (21 °C) and humidity (60%), under a fixed 12-h light/dark cycle, with free access to food and water.

Genotyping

All animals used were genotyped using a KAPA2G Fast HotStart DNA polymerase kit from Kapa Biosystem. Primers used were as follows: PINK-1 WT upper primer (0.2 μM) CCCTCTATGGCGTCCTCTT and PINK-1 WT lower primer (0.2 μM) CAGCAACTGCAAGGTCATCA; PINK-1-KO mouse upper primer (0.2 μM) GCACCCTGACCTTGGTTCCTA and PINK-1-KO mouse lower primer (0.2 μM) GGGGGAACTTCCTGACTAGG; PARKIN WT upper primer (1 μM) TGCTCTGGGGTTCGTC and PARKIN WT lower primer (1 μM) TCCACTGGCAGAGTAAATGT; DJ1 WT upper primer (0.5 μM) TGGTGAAGTGAGCAGACAGG and DJ1 WT lower primer (0.5 μM) AGGAGCCAAAGAAACAAGCA; and Parkin (0.25 μM) or DJ-1 (0.5 μM) Neo upper primer CCTGCTTGCCGAATATCAT and Parkin (0.25 μM) or DJ-1 (0.5 μM) Neo lower primer AAGGCGATAGAAGGCGATG.

Primary neuronal cultures and drug treatments

Cultures were prepared according to a previously described protocol (53), with minor variations (9). Dissociated neurons microdissected from the SNc or VTA of postnatal day 0–2 (P0–P2) Parkin-KO mice (48), Pink1-KO mice (54), or DJ-1-KO mice (40) were seeded on a monolayer of corresponding cortical astrocytes grown on collagen/poly-L-lysine–coated glass coverslips. The total seeded neuron density was 100,000 cells/ml for all experiments, except for the metabolic flux experiments for which the density was 250,000 cells/ml. All cultures were incubated at 37 °C in 5% CO_2 and maintained in 2/3 of Neurobasal™-A medium enriched with 1% penicillin/streptomycin, 1% Glutamax™-1, 2% B-27 supplement, and 5% fetal bovine serum (Invitrogen) plus 1/3 of minimum essential medium enriched with 1% penicillin/streptomycin, 1% Glutamax™-1, 20 mM glucose, 1 mM sodium pyruvate, and 100 μl of MITO+ serum extender. In some experiments, MPP+ (Sigma) (5 or 10 μM) or H_2O_2 (Sigma) (100–150 μM) were added at 10 DIV for 24 h. In other experiments, the complex I blocker rotenone (Sigma) (50 nM) was added at 8 DIV for 72 h. For the rescue experiments, AAV encoding GFP (AAV-CBA-emGFP) or WT Parkin fused with GFP (AAV-CBA-emGFP-FLAG-Parkin WT) was applied to the cells the day of the culture, leading to infection of more than 95% of the cells.

Metabolic flux experiments

The rate of oxygen consumption derived from mitochondrial OXPHOS and the ECAR derived from glycolysis were assessed using an extracellular flux analyzer (Seahorse Biosciences), as described previously (9). Cells were plated on XF24 tissue culture plates and maintained in culture for 5 or 10 days. Before experiments, cells were incubated for 1 h at 37 °C in a CO_2-free incubator in bicarbonate-free Dulbecco's modified Eagle's medium (Sigma) supplemented with 2 mM GlutaMax™-1 (Invitrogen), 1 mM sodium pyruvate (Sigma), 25 mM D-glucose (Sigma), 63.3 mM NaCl (Sigma), and phenol red (Sigma). The pH was adjusted to 7.4 with NaOH. These concentrations of substrate represent saturating concentrations to ensure that they did not limit the rate of respiration and glycolysis. Oxygen consumption was sequentially measured under basal conditions, in the presence of the mitochondrial uncoupler CCCP (0.5 μM), to assess the maximal oxidative capacity and in the presence of the mitochondrial inhibitors rotenone (1 μM) and antimycin A (1 μM) to assess non-mitochondrial oxygen consumption. After the assays, the cells were immediately fixed for immunofluorescence. For 10 DIV cultures, the OCR was normalized to cell number, as assessed by DAPI staining. Because neurons were cultured together with astrocytes, parallel measurements were also performed from pure astrocyte cultures. After subtraction of the OCR measured from astrocytes, the resulting OCR values measured from mixed cultures were normalized in a second step on the total number of neurons identified with MAP-2 immunostaining. For 5 DIV cultures, OCR and all ECAR measurements, the contribution of glial cells was not subtracted because values in co-cultures were close to those of astrocytes. Values were normalized on total cell number and then on the total number of neurons.

Immunofluorescence

Cultures were fixed for 30 min with 4% paraformaldehyde in PBS and permeabilized, and nonspecific binding sites were blocked. Cells were incubated overnight with a primary antibody solution containing 1% bovine serum albumin (BSA), 0.1% Triton X-100 in PBS, 5% goat serum, and 0.02% NaN^3. Cells were washed several times in PBS before incubation for 1 h with the appropriate Alexa-labeled secondary antibodies (Invitrogen). Primary antibodies used were TH-rabbit (Millipore, 1:2000), MAP-2–mouse (Chemicon, 1:1000), and RFP-rabbit (Rockland, 1:1000).

Mitochondrial network quantification

Mitochondria were labeled by infecting neurons with a lentivirus encoding DsRed2-mito (mitochondrially-targeted red fluorescent reporter protein) at 30 multiplicities of infection at the time of plating and fixed at 10 DIV. Images were obtained by capturing confocal 0.5-μm z-stacks (10–15 images) using a ×60 oil-immersion objective (NA 1.42) on a Olympus Fluoview FV1000 confocal using Fluoview version 3.1b software. Image analysis was performed using ImageJ software. Only TH-positive infected DA neurons were selected for analysis. Regions of interest were determined to separately measure DsRed2-mito signal in the cell body, isolated dendrite segments, and isolated axon segments. The percentage of TH-positive area covered by DsRed signal was measured in each cellular compartment.

Global neuronal morphology and survival assessment

At 10 DIV, TH-positive axonal arborization surface was estimated by capturing five confocal image stacks per coverslip randomly throughout the coverslip with a ×20 water immersion objective (NA 0.5). Using a homemade macro in ImageJ, MAP2 and TH signals were thresholded to remove background and then binarized. MAP2 signal area was then removed from TH signal area, and the remaining axonal signal surface was measured. For survival assessment, the number of TH neurons with clear round nuclei on the coverslip were estimated by scanning the coverslip vertically and horizontally (cross-counting) with a ×20 dry objective (NA 0.40) on a Nikon Eclipse TE200 inverted microscope.

Parkin-KO mouse glial cell proliferation measurements

Glial cells were grown on coverslips for 1, 3, 7, and 10 DIV. On a separate series of coverslips, FUDR was added once the glial cell reached confluence as is typically performed for neuronal cultures. The number of glial cells was measured by counting cells in five random pictures per coverslip after DAPI staining.

Measurement of total cellular ATP

Cellular ATP content was determined using the "ATPlite" kit (PerkinElmer Life Sciences) according to the manufacturer's instructions. The cells were collected by trypsinization and centrifugation at 500 × *g* and then resuspended in PBS, pH 7.4. Measurements were performed on a Wallac Victor plate reader (PerkinElmer Life Sciences). One coverslip from each sample was labeled with DAPI to quantify total cell number. ATP values were then normalized on total cell number. Oligomycin-insensitive ATP production (from glycolysis) was subtracted. Values obtained from measurements from glial cells alone were subtracted. The remaining values, representing the ATP derived from OXPHOS in neurons only, were then normalized on the total number of neurons identified with MAP-2 immunostaining.

Radioligand assay

10 DIV cultures were incubated with trypsin at 37 °C for 10 min and collected in 20% FBS in PBS after subsequent centrifugation at 900 and 1500 × *g* for 5 min. One ml of PBS was added between the two centrifugations. The cell pellets were resuspended in 200 μl of a cold binding buffer solution (Na_2HPO_4 10.1 mM, KH_2PO_4 1.8 mM, KCl 2 mM, NaCl 137 mM) and then stored at −80 °C until use. Tissue homogenates were washed by centrifugation at 13,000 × *g* (4 °C) for 15 min. Supernatants were discarded, and pellets were resuspended in the same buffer. DAT labeling was performed by adding 20 pM [^{125}I]RTI-55 ligand (specific activity, 2200 Ci/mmol, PerkinElmer Life Sciences, Woodbride, Ontario, Canada) to the tissue homogenates in a final volume of 200 μl. Each sample was evaluated in triplicate. Nonspecific binding was estimated in the presence of 1 μM of the selective DA reuptake inhibitor GBR12909 (Sigma). Incubation at room temperature for 1 h was terminated by rapid filtration through Whatman GF/C glass filters under vacuum, followed by three rinses (4 ml each) with the same ice-cold buffer. Radioactivity was counted by γ scintigraphy.

Statistics

Parametric statistical tests were used because samples contained data with normal distributions. Data were always obtained from a minimum of three separate sets of experiments and presented as mean ± S.E. The level of statistical significance was established at $p < 0.05$ in one- or two-way analyses of variance or two-tailed *t* tests. A ROUT outlier analysis was performed when needed ($Q = 1\%$). Statistical analyses were performed with the Prism 7 software (GraphPad Software, * = $p <$ 0.05; ** = $p < 0.01$; *** = $p < 0.001$; and **** = $p < 0.0001$). The Tukey post hoc test was used when all the means were compared with each other, and the Sidak post hoc test was used when only subsets of means were compared.

Author contributions—N. G., C. P., C. S., D. M., and D. L. formal analysis; N. G., C. P., C. S., M.-J. B., D. M., and D. L. investigation; N. G., C. P., M.-J. B., and D. L. methodology; N. G. and L.-E. T. writing-original draft; N. G., C. P., and L.-E. T. writing-review and editing; R. S. S., D. S. P., and L.-E. T. conceptualization; R. S. S., D. S. P., and L.-E. T. resources; R. S. S., D. S. P., and L.-E. T. funding acquisition; R. S. S., D. S. P., and L.-E. T. project administration; L.-E. T. data curation; L.-E. T. supervision; L.-E. T. validation.

Acknowledgment—The Central Nervous System Research Group is supported by an infrastructure grant from the Fonds du Québec en Recherche, Santé (FRQS).

References

1. De Rosa, P., Marini, E. S., Gelmetti, V., and Valente, E. M. (2015) Candidate genes for Parkinson disease: lessons from pathogenesis. *Clin. Chim. Acta* **449,** 68–76 CrossRef Medline
2. Parent, M., and Parent, A. (2006) Relationship between axonal collateralization and neuronal degeneration in basal ganglia. *J. Neural Transm. Suppl.* **2006,** 85–88 Medline
3. Matsuda, W., Furuta, T., Nakamura, K. C., Hioki, H., Fujiyama, F., Arai, R., and Kaneko, T. (2009) Single nigrostriatal dopaminergic neurons form widely spread and highly dense axonal arborizations in the neostriatum. *J. Neurosci.* **29,** 444–453 CrossRef Medline
4. Bolam, J. P., and Pissadaki, E. K. (2012) Living on the edge with too many mouths to feed: why dopamine neurons die. *Mov. Disord.* **27,** 1478–1483 CrossRef Medline
5. Gauthier, J., Parent, M., Lévesque, M., and Parent, A. (1999) The axonal arborization of single nigrostriatal neurons in rats. *Brain Res.* **834,** 228–232 CrossRef Medline
6. Perier, C., and Vila, M. (2012) Mitochondrial biology and Parkinson's disease. *Cold Spring Harb. Perspect. Med.* **2,** a009332 Medline
7. Franco-Iborra, S., and Perier, C. (2015) Neurodegeneration: the size takes it all. *Curr. Biol.* **25,** R797–R800 CrossRef Medline
8. Pissadaki, E. K., and Bolam, J. P. (2013) The energy cost of action potential propagation in dopamine neurons: clues to susceptibility in Parkinson's disease. *Front. Comput. Neurosci.* **7,** 13 Medline
9. Pacelli, C., Giguère, N., Bourque, M.-J., Lévesque, M., Slack, R. S., and Trudeau, L.-É. (2015) Elevated mitochondrial bioenergetics and axonal arborization size are key contributors to the vulnerability of dopamine neurons. *Curr. Biol.* **25,** 2349–2360 CrossRef Medline
10. Yamano, K., Matsuda, N., and Tanaka, K. (2016) The ubiquitin signal and autophagy: an orchestrated dance leading to mitochondrial degradation. *EMBO Rep.* **17,** 300–316 CrossRef Medline
11. Pickrell, A. M., Huang, C.-H., Kennedy, S. R., Ordureau, A., Sideris, D. P., Hoekstra, J. G., Harper, J. W., and Youle, R. J. (2015) Endogenous Parkin preserves dopaminergic substantia nigral neurons following mitochondrial DNA mutagenic stress. *Neuron* **87,** 371–381 CrossRef Medline
12. McLelland, G.-L., Soubannier, V., Chen, C. X., McBride, H. M., and Fon, E. A. (2014) Parkin and PINK1 function in a vesicular trafficking pathway regulating mitochondrial quality control. *EMBO J.* **33,** 282–295 Medline
13. Solano, R. M., Casarejos, M. J., Menéndez-Cuervo, J., Rodriguez-Navarro, J. A., García de Yébenes, J., and Mena, M. A. (2008) Glial dysfunction in parkin null mice: effects of aging. *J. Neurosci.* **28,** 598–611 CrossRef Medline
14. Javitch, J. A., D'Amato, R. J., Strittmatter, S. M., and Snyder, S. H. (1985) Parkinsonism-inducing neurotoxin, *N*-methyl-4-phenyl-1,2,3,6-tetrahydropyridine: uptake of the metabolite *N*-methyl-4-phenylpyridine by dopamine neurons explains selective toxicity. *Proc. Natl. Acad. Sci. U.S.A.* **82,** 2173–2177 CrossRef Medline
15. Rousseaux, M. W., Marcogliese, P. C., Qu, D., Hewitt, S. J., Seang, S., Kim, R. H., Slack, R. S., Schlossmacher, M. G., Lagace, D. C., Mak, T. W., and

Park, D. S. (2012) Progressive dopaminergic cell loss with unilateral-to-bilateral progression in a genetic model of Parkinson disease. *Proc. Natl. Acad. Sci. U.S.A.* **109,** 15918–15923 CrossRef Medline

16. Stevens, D. A., Lee, Y., Kang, H. C., Lee, B. D., Lee, Y.-I., Bower, A., Jiang, H., Kang, S.-U., Andrabi, S. A., Dawson, V. L., Shin, J.-H., and Dawson, T. M. (2015) Parkin loss leads to PARIS-dependent declines in mitochondrial mass and respiration. *Proc. Natl. Acad. Sci. U.S.A.* **112,** 11696–11701 CrossRef Medline
17. Lee, Y., Stevens, D. A., Kang, S.-U., Jiang, H., Lee, Y.-I., Ko, H. S., Scarffe, L. A., Umanah, G. E., Kang, H., Ham, S., Kam, T.-I., Allen, K., Brahmachari, S., Kim, J. W., Neifert, S., *et al.* (2017) PINK1 Primes Parkin-mediated ubiquitination of PARIS in dopaminergic neuronal survival. *Cell Rep.* **18,** 918–932 CrossRef Medline
18. Hauser, D. N., and Hastings, T. G. (2013) Mitochondrial dysfunction and oxidative stress in Parkinson's disease and monogenic parkinsonism. *Neurobiol. Dis.* **51,** 35–42 CrossRef Medline
19. Dias, V., Junn, E., and Mouradian, M. M. (2013) The role of oxidative stress in Parkinson's disease. *J. Parkinsons Dis.* **3,** 461–491 Medline
20. Zhang, W., Wang, T., Pei, Z., Miller, D. S., Wu, X., Block, M. L., Wilson, B., Zhang, W., Zhou, Y., Hong, J.-S., and Zhang, J. (2005) Aggregated α-synuclein activates microglia: a process leading to disease progression in Parkinson's disease. *FASEB J.* **19,** 533–542 CrossRef Medline
21. Canet-Avilés, R. M., Wilson, M. A., Miller, D. W., Ahmad, R., McLendon, C., Bandyopadhyay, S., Baptista, M. J., Ringe, D., Petsko, G. A., and Cookson, M. R. (2004) The Parkinson's disease protein DJ-1 is neuroprotective due to cysteine-sulfinic acid-driven mitochondrial localization. *Proc. Natl. Acad. Sci. U.S.A.* **101,** 9103–9108 CrossRef Medline
22. Greene, J. C., Whitworth, A. J., Kuo, I., Andrews, L. A., Feany, M. B., and Pallanck, L. J. (2003) Mitochondrial pathology and apoptotic muscle degeneration in *Drosophila* parkin mutants. *Proc. Natl. Acad. Sci. U.S.A.* **100,** 4078–4083 CrossRef Medline
23. Luk, K. C., Rymar, V. V., van den Munckhof, P., Nicolau, S., Steriade, C., Bifsha, P., Drouin, J., and Sadikot, A. F. (2013) The transcription factor Pitx3 is expressed selectively in midbrain dopaminergic neurons susceptible to neurodegenerative stress. *J. Neurochem.* **125,** 932–943 CrossRef Medline
24. Hung, H. C., and Lee, E. H. (1996) The mesolimbic dopaminergic pathway is more resistant than the nigrostriatal dopaminergic pathway to MPTP and MPP+ toxicity: role of BDNF gene expression. *Brain Res. Mol. Brain Res.* **41,** 14–26 Medline
25. Ren, Y., Jiang, H., Hu, Z., Fan, K., Wang, J., Janoschka, S., Wang, X., Ge, S., and Feng, J. (2015) Parkin mutations reduce the complexity of neuronal processes in iPSC-derived human neurons. *Stem Cells* **33,** 68–78 CrossRef Medline
26. Burman, J. L., Yu, S., Poole, A. C., Decal, R. B., and Pallanck, L. (2012) Analysis of neural subtypes reveals selective mitochondrial dysfunction in dopaminergic neurons from parkin mutants. *Proc. Natl. Acad. Sci. U.S.A.* **109,** 10438–10443 CrossRef Medline
27. Damiano, M., Gautier, C. A., Bulteau, A.-L., Ferrando-Miguel, R., Gouarne, C., Paoli, M. G., Pruss, R., Auchère, F., L'Hermitte-Stead, C., Bouillaud, F., Brice, A., Corti, O., and Lombès, A. (2014) Tissue- and cell-specific mitochondrial defect in Parkin-deficient mice. *PLoS One* **9,** e99898 CrossRef Medline
28. Cao, X., Wang, H., Wang, Z., Wang, Q., Zhang, S., Deng, Y., and Fang, Y. (2017) *In vivo* imaging reveals mitophagy independence in the maintenance of axonal mitochondria during normal aging. *Aging Cell* **16,** 1180–1190 CrossRef Medline
29. Pacelli, C., De Rasmo, D., Signorile, A., Grattagliano, I., di Tullio, G., D'Orazio, A., Nico, B., Comi, G. P., Ronchi, D., Ferranini, E., Pirolo, D., Seibel, P., Schubert, S., Gaballo, A., Villani, G., and Cocco, T. (2011) Mitochondrial defect and PGC-1α dysfunction in parkin-associated familial Parkinson's disease. *Biochim. Biophys. Acta* **1812,** 1041–1053 CrossRef Medline
30. Palacino, J. J., Sagi, D., Goldberg, M. S., Krauss, S., Motz, C., Wacker, M., Klose, J., and Shen, J. (2004) Mitochondrial dysfunction and oxidative damage in parkin-deficient mice. *J. Biol. Chem.* **279,** 18614–18622 CrossRef Medline
31. McWilliams, T. G., Prescott, A. R., Montava-Garriga, L., Ball, G., Singh, F., Barini, E., Muqit, M. M. K., Brooks, S. P., and Ganley, I. G. (2018) Basal mitophagy occurs independently of PINK1 in mouse tissues of high metabolic demand. *Cell Metab.* **27,** 439–449.e5 CrossRef Medline
32. Yao, Z., Gandhi, S., Burchell, V. S., Plun-Favreau, H., Wood, N. W., and Abramov, A. Y. (2011) Cell metabolism affects selective vulnerability in PINK1-associated Parkinson's disease. *J. Cell Sci.* **124,** 4194–4202 CrossRef Medline
33. Heo, J. Y., Park, J. H., Kim, S. J., Seo, K. S., Han, J. S., Lee, S. H., Kim, J. M., Park, J. I., Park, S. K., Lim, K., Hwang, B. D., Shong, M., and Kweon, G. R. (2012) DJ-1 null dopaminergic neuronal cells exhibit defects in mitochondrial function and structure: involvement of mitochondrial complex I assembly. *PLoS One* **7,** e32629 CrossRef Medline
34. Gispert, S., Ricciardi, F., Kurz, A., Azizov, M., Hoepken, H.-H., Becker, D., Voos, W., Leuner, K., Müller, W. E., Kudin, A. P., Kunz, W. S., Zimmermann, A., Roeper, J., Wenzel, D., Jendrach, M., *et al.* (2009) Parkinson phenotype in aged PINK1-deficient mice is accompanied by progressive mitochondrial dysfunction in absence of neurodegeneration. *PLoS ONE* **4,** e5777 CrossRef Medline
35. Paterna, J.-C., Leng, A., Weber, E., Feldon, J., and Büeler, H. (2007) DJ-1 and Parkin modulate dopamine-dependent behavior and inhibit MPTP-induced nigral dopamine neuron loss in mice. *Mol. Ther.* **15,** 698–704 CrossRef Medline
36. Benskey, M. J., Manfredsson, F. P., Lookingland, K. J., and Goudreau, J. L. (2015) The role of parkin in the differential susceptibility of tuberoinfundibular and nigrostriatal dopamine neurons to acute toxicant exposure. *Neurotoxicology* **46,** 1–11 CrossRef Medline
37. Rappold, P. M., and Tieu, K. (2010) Astrocytes and therapeutics for Parkinson's disease. Neurotherapeutics **7,** 413–423 CrossRef Medline
38. Nakajima, K., Hida, H., Shimano, Y., Fujimoto, I., Hashitani, T., Kumazaki, M., Sakurai, T., and Nishino, H. (2001) GDNF is a major component of trophic activity in DA-depleted striatum for survival and neurite extension of DAergic neurons. *Brain Res.* **916,** 76–84 CrossRef Medline
39. Shaltouki, A., Sivapatham, R., Pei, Y., Gerencser, A. A., Momčilović, O., Rao, M. S., and Zeng, X. (2015) Mitochondrial alterations by PARKIN in dopaminergic neurons using PARK2 patient-specific and PARK2 knockout isogenic iPSC lines. *Stem Cell Rep.* **4,** 847–859 CrossRef Medline
40. Kim, R. H., Smith, P. D., Aleyasin, H., Hayley, S., Mount, M. P., Pownall, S., Wakeham, A., You-Ten, A. J., Kalia, S. K., Horne, P., Westaway, D., Lozano, A. M., Anisman, H., Park, D. S., and Mak, T. W. (2005) Hypersensitivity of DJ-1-deficient mice to 1-methyl-4-phenyl-1,2,3,6-tetrahydropyrindine (MPTP) and oxidative stress. *Proc. Natl. Acad. Sci. U.S.A.* **102,** 5215–5220 CrossRef Medline
41. Haque, M. E., Mount, M. P., Safarpour, F., Abdel-Messih, E., Callaghan, S., Mazerolle, C., Kitada, T., Slack, R. S., Wallace, V., Shen, J., Anisman, H., and Park, D. S. (2012) Inactivation of Pink1 gene *in vivo* sensitizes dopamine-producing neurons to 1-methyl-4-phenyl-1,2,3,6-tetrahydropyridine (MPTP) and can be rescued by autosomal recessive Parkinson disease genes, Parkin or DJ-1. *J. Biol. Chem.* **287,** 23162–23170 CrossRef Medline
42. Martinat, C., Shendelman, S., Jonason, A., Leete, T., Beal, M. F., Yang, L., Floss, T., and Abeliovich, A. (2004) Sensitivity to oxidative stress in DJ-1-deficient dopamine neurons: an ES-derived cell model of primary Parkinsonism. *PLoS Biol.* **2,** e327 CrossRef Medline
43. Inden, M., Taira, T., Kitamura, Y., Yanagida, T., Tsuchiya, D., Takata, K., Yanagisawa, D., Nishimura, K., Taniguchi, T., Kiso, Y., Yoshimoto, K., Agatsuma, T., Koide-Yoshida, S., Iguchi-Ariga, S. M., Shimohama, S., and Ariga, H. (2006) PARK7 DJ-1 protects against degeneration of nigral dopaminergic neurons in Parkinson's disease rat model. *Neurobiol. Dis.* **24,** 144–158 CrossRef Medline
44. Mullett, S. J., and Hinkle, D. A. (2009) DJ-1 knock-down in astrocytes impairs astrocyte-mediated neuroprotection against rotenone. *Neurobiol. Dis.* **33,** 28–36 CrossRef Medline
45. Lev, N., Barhum, Y., Ben-Zur, T., Melamed, E., Steiner, I., and Offen, D. (2013) Knocking out DJ-1 attenuates astrocytes neuroprotection against 6-hydroxydopamine toxicity. *J. Mol. Neurosci.* **50,** 542–550 CrossRef Medline
46. Aguiar, A. S., Jr., Tristão, F. S., Amar, M., Chevarin, C., Lanfumey, L., Mongeau, R., Corti, O., Prediger, R. D., and Raisman-Vozari, R. (2013)

Parkin-knockout mice did not display increased vulnerability to intranasal administration of 1-methyl-4-phenyl-1,2,3,6-tetrahydropyridine (MPTP). *Neurotox. Res.* **24,** 280–287 CrossRef Medline

47. Thomas, B., von Coelln, R., Mandir, A. S., Trinkaus, D. B., Farah, M. H., Leong Lim, K., Calingasan, N. Y., Flint Beal, M., Dawson, V. L., and Dawson, T. M. (2007) MPTP and DSP-4 susceptibility of substantia nigra and locus coeruleus catecholaminergic neurons in mice is independent of parkin activity. *Neurobiol. Dis.* **26,** 312–322 CrossRef Medline
48. Itier, J.-M., Ibanez, P., Mena, M. A., Abbas, N., Cohen-Salmon, C., Bohme, G. A., Laville, M., Pratt, J., Corti, O., Pradier, L., Ret, G., Joubert, C., Periquet, M., Araujo, F., Negroni, J., *et al.* (2003) Parkin gene inactivation alters behaviour and dopamine neurotransmission in the mouse. *Hum. Mol. Genet.* **12,** 2277–2291 CrossRef Medline
49. Perez, F. A., Curtis, W. R., and Palmiter, R. D. (2005) Parkin-deficient mice are not more sensitive to 6-hydroxydopamine or methamphetamine neurotoxicity. *BMC Neurosci.* **6,** 71 CrossRef Medline
50. Jiang, H., Ren, Y., Yuen, E. Y., Zhong, P., Ghaedi, M., Hu, Z., Azabdaftari, G., Nakaso, K., Yan, Z., and Feng, J. (2012) Parkin controls dopamine utilization in human midbrain dopaminergic neurons derived from induced pluripotent stem cells. *Nat. Commun.* **3,** 668 CrossRef Medline
51. Casarejos, M. J., Menéndez, J., Solano, R. M., Rodríguez-Navarro, J. A., García de Yébenes, J., and Mena, M. A. (2006) Susceptibility to rotenone is increased in neurons from parkin null mice and is reduced by minocycline. *J. Neurochem.* **97,** 934–946 CrossRef Medline
52. Haque, M. E., Thomas, K. J., D'Souza, C., Callaghan, S., Kitada, T., Slack, R. S., Fraser, P., Cookson, M. R., Tandon, A., and Park, D. S. (2008) Cytoplasmic Pink1 activity protects neurons from dopaminergic neurotoxin MPTP. *Proc. Natl. Acad. Sci. U.S.A.* **105,** 1716–1721 CrossRef Medline
53. Fasano, C., Thibault, D., and Trudeau, L. E. (2008) Culture of postnatal mesencephalic dopamine neurons on an astrocyte monolayer. *Curr. Protoc.* Neurosci. Chapter 3, Unit 3.21 CrossRef Medline
54. Akundi, R. S., Huang, Z., Eason, J., Pandya, J. D., Zhi, L., Cass, W. A., Sullivan, P. G., and Büeler, H. (2011) Increased mitochondrial calcium sensitivity and abnormal expression of innate immunity genes precede dopaminergic defects in Pink1-deficient mice. *PLoS One* **6,** e16038 CrossRef Medline